

1 **Colder and drier winter conditions are associated with greater SARS-CoV-2 transmission: a**  
2 **regional study of the first epidemic wave in north-west hemisphere countries.**

3

4

Version 1, 26 January 2021

5

6 Jordi Landier<sup>1\*</sup>, Juliette Paireau<sup>2,3</sup>, Stanislas Rebaudet<sup>1,4</sup>, Eva Legendre<sup>1</sup>, Laurent Lehot<sup>1</sup>, Arnaud  
7 Fontanet<sup>5,6</sup>, Simon Cauchemez<sup>2</sup>, Jean Gaudart<sup>7</sup>

8

9

10 <sup>1</sup> IRD, Aix Marseille Univ, INSERM, SESSTIM, Marseille, France.

11 <sup>2</sup> Mathematical Modelling of Infectious Diseases Unit, Institut Pasteur, UMR2000, CNRS, Paris, France.

12 <sup>3</sup> Santé publique France, French National Public Health Agency, Saint Maurice, France

13 <sup>4</sup> Hôpital Européen Marseille, France.

14 <sup>5</sup> Emerging Infectious Diseases Unit, Institut Pasteur, Paris, France.

15 <sup>6</sup> PACRI Unit, Conservatoire National des Arts et Métiers, Paris, France.

16 <sup>7</sup> Aix Marseille Univ, APHM, INSERM, IRD, SESSTIM, Hop Timone, BioSTIC, Marseille, France.

17

18 \* corresponding author, [jordi.landier@ird.fr](mailto:jordi.landier@ird.fr)

19 **Abstract**

20 Higher transmissibility of SARS-CoV-2 in cold and dry weather conditions has been hypothesized since  
21 the onset of the COVID-19 pandemic but the level of epidemiological evidence remains low.

22 During the first wave of the pandemic for Spain, Italy, France, Portugal, Canada and USA presented an  
23 early spread, a heavy COVID-19 burden, and low initial public health response until lockdowns. We  
24 used regional death counts as a proxy for infections while diagnostic tests remained limited and  
25 calculated a basic reproduction number (R0) in 63 regions. After adjusting for population density, early  
26 spread of the epidemic, and aged population, temperature and humidity were negatively associated  
27 to SARS-CoV-2 transmissibility. A -1g/m<sup>3</sup> lower mean absolute humidity was associated with a 0.15-  
28 unit higher R0. Below 10°C, a 1°C-higher temperature was associated with a 0.16-unit lower R0.

29 Our results confirm a strong dependency of SARS-CoV-2 transmissibility to weather conditions in the  
30 absence of control measures. The initiation of the second wave in north-west hemisphere countries  
31 was likely triggered by the transition from summer- to winter-like conditions. High levels of restrictions  
32 to social activities should be maintained until spring to avoid or limit a third wave.

**NOTE: This preprint reports new research that has not been certified by peer review and should not be used to guide clinical practice.**

## 1 Introduction

2

3 The spread of SARS-CoV-2 in February-March 2020 caught the majority of European and North  
4 American countries unprepared. The spread of the virus was largely uncontrolled until movement  
5 restriction and social distancing policies were put in place at national or regional level with various  
6 degrees of intensity [1]. Most regions experienced a peak in hospital admissions, approximately 2  
7 weeks after lockdown was imposed, corresponding to infections acquired around the date of  
8 lockdown [2].

9 The spread of this first wave was largely heterogeneous between countries. Various determinants  
10 were proposed to explain the differential spread of the virus. Asian countries (Japan, South Korea,  
11 Vietnam and Thailand) and isolated countries (Australia, New Zealand, Iceland) experienced only  
12 limited transmission and stood out for high levels of preparedness and efficient response strategies.  
13 Even within South West European and North American countries where no effective response was  
14 deployed before lockdowns, SARS-CoV-2 virus spread heterogeneously at the regional level, as  
15 observed from hospitalization, death counts, and confirmed by serological surveys [3, 4].

16 Epidemic spread is characterized by the basic reproduction number, or  $R_0$ .  $R_0$  expresses the number  
17 of secondary cases resulting from a given case in the context of a naive population with uniform  
18 probability of contact.

19  $R_0$  depends on individual susceptibility to infection when in contact with an infective individual, and  
20 on the probability of an infectious contact. Environmental parameters affect  $R_0$ : population density  
21 increases the probability of contacts between individuals and weather conditions may affect the  
22 survival of the virus or the individual susceptibility to an infection. Most known respiratory viruses  
23 spread during the cold season in the temperate Northern hemisphere [5]. Weather conditions in  
24 winter can also affect individual susceptibility to infection through irritation of the nasal mucosa, but  
25 also influence the behaviour of individuals towards conditions prone to transmission (living or  
26 gathering in closed, heated spaces with a dry atmosphere) [5]. In addition, temperature, humidity,  
27 and UV, might directly affect the virus survival and modify infectiousness [6, 7]. Individual preventive  
28 behaviours (masks), collective strategies reducing mobility and contacts (lockdowns) or limiting the  
29 duration of the infectious period (detection and isolation) modify the number of secondary cases and  
30 the effective reproduction number can be calculated, which accounts for these alterations in the  
31 “natural” history of transmission.

32 In spite of a large number of studies, the evidence regarding the link between weather conditions and  
33 SARS-CoV-2 transmission remains limited. At date of 15 May 2020, a systematic review retained 61  
34 studies analysing the relationship between COVID-19 epidemic and environmental factors [8].  
35 Methodological issues included the lack of controlling for confounding factors such as population  
36 density [8]. Inappropriate epidemiological and statistical methods were also pointed out [8, 9].  
37 Comparison between countries with different counter epidemic responses, testing strategy, or delayed  
38 onset of the epidemic might also have led to inconsistent results [8]. An earlier review retaining 17  
39 studies highlighted the risk of bias and the low level of available evidence [10]. Between 15 May 2020  
40 and 15 December 2020, our systematic search identified 82 research articles, of which only 15 (18%)  
41 analysed the growth rate or the reproduction number of SARS-CoV-2 (Appendix p2). Only four studies  
42 of climate and reproduction number included adjustments for confounding factors, and three of four  
43 included relevant covariates of population mobility, population density, and took into account  
44 interventions when necessary [11–13]. Of these, two were conducted over small geographical units:  
45 one study of 212 US counties identified a negative relationship between temperature increase and

1 SARS-CoV-2 growth, while the other study including 28 Japanese prefectures identified a positive  
2 relationship [11, 12]. The third study was at the global scale for 203 states (USA, Canada, Australia and  
3 China) or countries and identified a negative association between UV light exposure and SARS-CoV-2  
4 growth. Temperature was negatively associated with growth only after adjustment for UV light  
5 exposure [13]. All three studies identified a positive association between population density and  
6 epidemic growth.

7 Overall, multiple studies described a negative relationship between temperature and COVID-19  
8 outcomes but the majority were unadjusted ecological correlation studies with strong risk of bias  
9 bringing low quality evidence [8], and evidence from multivariable growth studies remains ambiguous.

10 A modelling study defined the range of possible dependency between SARS-CoV-2 transmission and  
11 absolute humidity, based on two known coronaviruses and influenza [14], and recent models still do  
12 not include specific SARS-CoV-2 data [15]. More precise estimations of the effect of meteorological  
13 conditions on the spread of SARS-CoV-2 are required to better anticipate and inform policies regarding  
14 seasonal adjustments [16].

15 The objective of this study was to evaluate the contribution of weather parameters in the transmission  
16 of SARS-CoV-2, by analysing their effect on SARS-CoV-2 basic reproduction number in a context of low  
17 public health response during the early phase of the first wave in 6 north-western hemisphere  
18 countries.

## 19 Material and methods

20

### 21 Study design

22 In order to compare the drivers of the epidemic dynamics between regions accurately, we calculated  
23 the basic reproduction number ( $R_0$ ) of the virus for each region affected by the first wave of COVID-19  
24 epidemic in six countries, using the dynamics of the daily death counts. These six countries were  
25 located in the western part of the northern hemisphere, approximately between 25 and 50° of latitude  
26 (Figure S2). These countries experienced winter conditions and underwent significant SARS-CoV-2  
27 transmission in a context of low public health response during the first wave of the epidemic.

28 This analysis was conducted at the first administrative subdivision country, here referred to as  
29 “region”. Regions corresponded to States in USA and Canada, autonomous communities in Spain, and  
30 regions in Italy (regioni), Portugal (região) and France (regions).

31 Confirmed case counts were insufficiently reliable due to overall lack of tests and different testing  
32 strategies between countries, between regions of the same country and between periods for the same  
33 region. Hospitalization counts were not available consistently at regional level across countries.  
34 Overall, COVID-19 deaths were preferred as they were less likely to have different definitions within  
35 the same region or country and to undergo significant changes over the study period.  $R_0$  is an indicator  
36 of the speed of progression of the outbreak, and was therefore less likely to be biased compared to  
37 indicators based on cumulative counts or cumulative incidence rates. Estimating  $R_0$  values based on  
38 deaths counts relies on the minimal assumption that the infection-fatality rate was constant over the  
39 study period (~1 month) for a given region, which defined a proportional relationship between  
40 infections and deaths.

41

## 1 **Study period**

2 Daily reporting of COVID-19 deaths was not initiated immediately after the first recorded deaths, and  
3 often started in a staggered manner in the different regions of a country. Analyses started on the date  
4 when 10 cumulative deaths were reached in a given region to account for these limitations of available  
5 data and to limit stochasticity in the occurrence of the first deaths.

6 This study aimed at estimating SARS-CoV-2  $R_0$  prior to implementation of major interventions in  
7 different regions. It was necessary to avoid the influence of the lockdown measures on the  
8 transmission. Reports indicated that symptoms occurred in median 5 days after infection (IQR=2-7),  
9 and hospitalization occurred in median 7 days after the onset of symptoms (IQR=3-9) [17, 18]. Reports  
10 of delay between hospitalization and death ranged from 5 days in New York to 12 days in Italy for  
11 patients admitted in ICU [19, 20]. In Spain and Italy, a median of 11 days (IQR=7-17), respectively 12  
12 days (IQR 7-20), were reported between onset of symptoms and death [21, 22], while an early study  
13 in China indicated a median of 18 days from onset of symptoms to death [23]. These figures lead to an  
14 overall estimation that deaths occurred in median 17-18 days after infection, with a broad range of  
15 variations. In France, mortality peaked at week 14 when lockdown occurred at the beginning of week  
16 12, i.e. for infections likely acquired during week 11. As a result, we initially assumed a 3-week delay  
17 between infection and death and excluded all data beyond 28 days from lockdown date to limit this  
18 study to deaths caused by pre-lockdown infections. We also conducted a more restrictive sensitivity  
19 analysis excluding all data beyond 18 days after lockdown date, which corresponded to the estimated  
20 median delay between infection and deaths.

21

## 22 **Inclusion criteria**

23 Regions where the smoothed daily death count did not rise above 5 deaths/day during the study period  
24 were not included in the analysis. Regions where the smoothed daily death count did not rise above  
25 10 deaths/day during the linear growth phase were excluded. This limited the study to regions having  
26 displayed a clear exponential growth phase.

27 One Italian region was excluded because there was no weather station data available except for 2  
28 stations >2000m altitude.

29

## 30 **Data**

### 31 **Deaths from COVID-19**

32 Regional level data on COVID-19 deaths were retrieved from data shared by national health ministries  
33 and/or public health agencies of Spain, Italy, Portugal, France, United States of America, and Canada  
34 (Table S1). Deaths were reported as daily new death counts or as a cumulative number.

35

### 36 **Population and geographical data**

37 Population structure by one- or five-year age groups, sex and region was retrieved from open access  
38 data shared by national institutes or administrations responsible for national statistics or demography  
39 (Table S1). The percentage of the region population aged  $\geq 70$  or  $\geq 80$  years was calculated in order to  
40 adjust for differences in way of life (e.g. rural regions have older population than metropolitan areas  
41 in Europe). The percentage of elderly inhabitants also represented an adjustment in case of a

1 differential spread of the epidemic among the elderly population (which would lead to a non-  
2 proportional increase in deaths compared to cases.

3 Region shapefiles by country were obtained from national geographical authorities, open source  
4 datasets or as provided in the coronavirus open data packages proposed by several national health  
5 agencies (Table S1). The region surface was either obtained from the geographical layer (land surface  
6 area), or calculated from the polygon extent. We estimated the percentage of each region surface with  
7  $\geq 5$  inhabitants per km<sup>2</sup> based on WorldPop 2020 raster dataset [24]. Population density was estimated  
8 as the population in the region divided by the surface after excluding areas  $< 5$  inhabitants/km<sup>2</sup> in order  
9 to limit the underestimation of population density when high heterogeneity existed between urban  
10 centers and sparsely populated territories within the same region (deserts, mountains, polar regions).

11

## 12 **Weather/climate**

13 Weather station reports since 1 January 2020 were obtained from US National Oceanic and  
14 Atmospheric Administration (NOAA) through the R-package {worldmet}. We extracted hourly  
15 temperature, relative humidity (RH), dew point (DP), precipitation and windspeed observations for  
16 each station. Hourly absolute humidity (AH, in g/m<sup>3</sup>) was calculated from RH and temperature based  
17 on the Clausius-Clapeyron formula [25]. Daily minimum, maximum and mean values were calculated  
18 for temperature, AH, RH, dew point, as well as cumulative sum of precipitation and mean wind speed.  
19 Days with  $\geq 5$  missing hourly record (no observation of any parameter) were excluded.

20 Each region was attributed stations based on geographic location. All available observations in weather  
21 stations of the region contributed to the regional daily average. Weather stations can be located in  
22 mountains or inhabited locations where they record weather conditions that differ strongly from  
23 actual populated areas of the same region. To avoid this bias, observations were assigned population-  
24 based weights: we estimated the population located within 10 km of each weather station using  
25 WorldPop 2020 data; and for each day and each region, we calculated the total population within 10km  
26 of any station reporting data for that day. Daily station observations were weighted in proportion of  
27 the population around each station relative to the total population. Stations located within 10-km of  
28 each other were included in a single buffer and each station was assigned equal weight within the  
29 buffer.

30 For each weather parameter, the regional summary value was calculated over the assumed  
31 transmission period. The assumed transmission period corresponded to the duration of the R0  
32 calculation period, lagged by 3 weeks. Sensitivity analyses included lags ranging from 2 to 8 weeks from  
33 R0 calculation period, i.e. -1 to +5 weeks from assumed transmission period. The longer lags were likely  
34 irrelevant for actual transmission but aimed at identifying climate rather than weather aspects.

35 Using this approach, the weather parameters averaged over the assumed transmission period and over  
36 each region included: minimum, mean and maximum average values for temperature, relative  
37 humidity, absolute humidity, dew point, average cumulative rainfall per day and average wind speed.

38

## 39 **Date of lockdown definition**

40 Lockdown date was defined using Google mobility data as the date when a decrease  $> 25\%$  in workplace  
41 localization was reported and sustained over 3 days in the region [26]. All references to a « date of  
42 lockdown » hereafter refer to this definition. This definition matched national lockdowns in European

1 countries. This simplification was necessary due to the heterogeneity in social distancing measures  
2 taken at regional (state) level in the USA and Canada. The objective was to exclude periods where  
3 transmission would start to slow down due to these measures.

4

#### 5 **Distance to first region with 10 cumulative deaths**

6 For each of the four European countries considered, the first region with 10 cumulative deaths was  
7 defined. In Portugal, two regions reached  $\geq 10$  deaths on the same day, and the region with the highest  
8 count (14 versus 12) was selected. Within each country, the euclidean distance in kilometers between  
9 the main city in each region and the main city in the first region above 10 cumulative deaths was  
10 calculated to reflect spatial autocorrelation due to proximity in the spread of the epidemic. In USA and  
11 Canada, distance to the first region above 10 cumulative deaths were calculated separately for East  
12 Coast and West Coast, using the limit between Central and Mountain time zones. This was necessary  
13 due to the early start of the epidemic in the state of Washington, which reached 10 deaths by 2 March  
14 2020, 16 days before the next state (New York on 18 March).

15

#### 16 **Statistical methods**

17 Statistical analyses were performed using R version 4.0. Maps were produced using ArcGIS 10.7.1.

18 Daily death counts were smoothed using a 5-day moving average filter to account for irregularities in  
19 data transmission and publication.

20 For each region, the exponential growth period was estimated using a  $\log(\text{deaths})=f(\text{time})$   
21 representation and  $r$  (the exponential growth rate) was extracted as the coefficient of a Poisson  
22 regression.  $R_0$  was calculated for each region using the generation time method assuming a gamma  
23 distribution with parameters 7 and 5.2 for SARS-CoV-2 generation time [27, 28]. In order to improve  
24 the adjustment of the regression, the start and end dates of calculation period were allowed to shift  
25 by up to 2 days (+/-1 day or +1/+2 days for start date if calculation period began at the date of 10  
26 cumulative deaths) using the built-in function `sensitivity.analysis()` of the package `{R0}` [29].

27 A directed acyclic graph (DAG) was constructed using Dagitty v3.0 web-based application  
28 (<http://www.dagitty.net/dags.html>) in order to visualise the relationships between  $R_0$  and the  
29 explanatory covariates (Figure S1). Dependence and independence assumptions were verified using  
30 Spearman correlation coefficient.

31 Relative humidity values are temperature-dependent and absolute humidity or dew point  
32 temperatures are also strongly correlated to temperature [30]. The different weather covariates  
33 observed at the same 3-week lag from  $R_0$  calculation period were included separately in the models.  
34 A generalized additive mixed model (gamm) regression was used to evaluate the effects of climate,  
35 population and other determinants on the value of  $R_0$ , using a Gaussian distribution and the identity  
36 link function (package `{mgcv}`). A country-level random effect was included to account for within-  
37 country correlations. Canada presented with only 2 regions and was grouped with USA for random  
38 effect, while the single region included from Portugal was grouped with Spain. Univariate analyses  
39 were conducted assuming linear and non-linear effects, using B-splines to model non-linear effect of  
40 covariates. Models were compared using the percentage of deviance explained and Akaike's  
41 Information Criterion.

1 We verified presence/absence of spatial autocorrelation in R0 values and in the final model residuals  
2 by calculating Moran's I.

3

#### 4 **Sensitivity analyses**

5 First, we assessed the importance of the 3-week delay for weather variables (corresponding to the  
6 delay between transmission period and R0 calculation period based on death count exponential  
7 growth). For this, we tested a variety of lags from -1 to 5 weeks from that estimated transmission  
8 period (*i.e.* 2 to 8 weeks from the R0 calculation period) and included them as linear explanatory  
9 variables in the univariable hierarchical model or as non-linear explanatory variables in the  
10 multivariable hierarchical generalised additive model.

11 Second, we assessed the effect of the 28-day window to define the exponential growth period by using  
12 a narrower window ending 18 days after date of lockdown. We recalculated R0 for regions where the  
13 linear growth period retained for the main analysis extended beyond the 18-day limit, and followed  
14 the same plan as the main analysis.

15 Third, we assessed possible continent specific effects by fitting continent-specific splines for weather  
16 variables in the final multivariate models.

## 17 **Results**

18

### 19 **Region selection**

20 The six countries (United States, Canada, Spain, Italy, France and Portugal) included 128 regions/states.  
21 Overseas regions (n=11) and regions which had experienced <10 cumulative deaths 28 days after  
22 lockdown (n=15) were not included (Figure 1). Likewise, regions with a maximal daily mortality <5  
23 deaths (n=19) within 28 days after lockdown were not included. Overall, 83 regions were assessed for  
24 exponential growth period, and R0 was calculated for 64 regions with sufficient exponential growth  
25 (Figure S2 in Appendix): 24 regions in the USA, 2 regions in Canada, 11 regions in France, 12 regions in  
26 Spain, 13 regions in Italy and 1 region in Portugal.

27

### 28 **Data description**

29 For regions analysed, the maximal daily death counts was 39 deaths/day in median (interquartile range  
30 (IQR)=18-83, max=779) and occurred in median 25 days (IQR=19-43) after the date of lockdown. Of  
31 note, larger reductions in human mobility patterns after lockdown as assessed from google mobility  
32 led to shorter delay (Spearman correlation coefficient = 0.63, p<0.0001, Figure S3). This delay was  
33 reduced to 19 days in median (IQR=17-27) for South European countries with nationwide lockdowns  
34 and strong mobility reductions (>60% in average, Figure S3).

35 R0 were estimated over a median exponential growth period of 11 days (IQR=9-14, range=5-19). In  
36 median, R0 estimation period started 5 days (IQR=0-8.5) and ended 16 days after the date of lockdown  
37 (IQR=11-21, range 1-27). Figure S4 presents details calculation periods.

38 The median R0 value was 2.58 (IQR=2.08-2.66). R0 estimates were lowest (<1.5) in two regions in  
39 France and one in Spain, USA and Italy (respectively in Centre-Val de Loire, Nouvelle Aquitaine, La  
40 Rioja, Alabama and Abruzzo). R0 were highest (>4.0) in New York (USA), Lombardia and Piemonte

1 (Italy), Castilla-La Mancha (Spain) and Ontario (Canada)(Figure 3A and B). Spain and Canada had overall  
2 higher R0 values compared to Italy, France and USA (Figure 4A). R0 values exhibited significant spatial  
3 autocorrelation (Moran's I=0.20, p=0.0087).

4 Covariates were heterogeneous between countries (Figure 3 and 4). Population density ranged  
5 between 82 and 1056 inhabitants/km<sup>2</sup> (median=271, Figure 3C and D) and was overall higher in Italy  
6 (Figure 4B). Mean absolute humidity during the estimated transmission period was 4.98 in median  
7 (IQR=4.29-5.99, range=2.26-11.32, Figure 3E and F) corresponding to a median dew point of 3.7°C  
8 (IQR=0.9-6.3, range=-7.7 – +15.3). Mean temperature was 9.8°C in median (IQR=7.1-11.5, range=-2.0-  
9 19.9). Distance to the first region with 10 cumulative deaths was 406km in median (IQR=228-794) and  
10 much larger in the USA compared to European countries (Figure 4F).

11

## 12 **Factors associated with R0**

13 Each variable was included in a univariate model assuming linear (Figure 5, Table S2) or non-linear  
14 (spline smoothing, Table S3) relationships with R0. We identified significant relationships between R0  
15 value and temperature, absolute humidity or dew point, average daily rainfall, but not with mean wind  
16 speed over the transmission period.

17 Multivariable models were constructed according to the DAG. After adjustment for distance to the  
18 nearest affected region, percentage of population over 80 and population density, there was a  
19 consistent relationship between increasing temperature, AH or dew point temperature, and  
20 decreasing R0. No relationship was found with average daily rainfall.

21 Mean temperature led to the model with the largest deviance explained compared to models including  
22 minimum or maximum temperature, or any AH or dew point temperature (Table 1). In this model, a  
23 10-fold (+1 log<sub>10</sub> unit) increase in population density was associated with a +0.67 R0 unit increase  
24 (95%CI=0.05-1.28). The proportion of population aged 80 years and older was not significantly  
25 associated with R0. The relationship between mean temperature and R0 was not linear. A strong,  
26 nearly linear drop of approximately 1.0 R0 unit was observed between 2.5 and 12°C, and a plateau  
27 beyond 12°C (Figure 6 and 7). The residuals from this model did not exhibit significant spatial  
28 autocorrelation (Moran's I=0.054, p=0.215).

29 Mean AH and mean dew point values exhibited similar profiles with increasing values associate with  
30 decreasing R0 values (Table 1, Figure 6). In spite of the narrower range of values, it seemed that the  
31 relationship between R0 and AH or dew point temperature did not reach a plateau (Figure 7). Assuming  
32 a linear relationship, a 1 g/m<sup>3</sup> higher absolute humidity translated in a 0.15 unit lower regional R0,  
33 respectively a 1°C higher dew point temperature translated in a 0.08 unit lower R0 (Table S5).

34

## 35 **Sensitivity analyses**

36 First, using lagged weather summary values as linear univariate predictors, our statistical model found  
37 similar relationships between R0 and temperature variables, but 0-, 1- and 5-week lags led to the  
38 strongest effect for mean AH and mean DP (Figure S5). Using lagged weather summary values as non-  
39 linear predictors in the multivariate model, the shapes of the relationships between temperature, AH  
40 and DP remained similar, with a nearly linear drop reaching a plateau at values corresponding to milder  
41 winter weather/climate (Figure S6). Overall, correlations were strong between weather summary  
42 observations at the different lags (Figure S7). Correlations of lagged temperature and humidity  
43 observations was highest between -1, 0, 1 and 5-week lagged observations compared to other lags.

1 Second, when limiting the R0 calculation window to 18-day after date of lockdown, 10 additional  
2 regions were excluded and analysis was conducted on 53 regions. After adjusting for population  
3 density, population over 80 and distance to the first region affected, the non-linear negative  
4 relationship between R0 and temperature remained unchanged, reaching a plateau around 10°C  
5 (spline p-value=0.0475). The shape of the relationship between AH, respectively DP, and R0 remained  
6 similar but did not reach statistical significance (p-value=0.19). Later AH or DP summary values,  
7 corresponding to 1 week later than the estimated transmission period (i.e. 2-week lag from R0  
8 calculation period), restored the negative relationship with R0 (p=0.0661, respectively p=0.0667).

9 Third, fitting continent-specific splines for weather covariates, also resulted in low statistical power:  
10 only 37 regions in South Europe and 26 in North America. After adjusting for population density,  
11 population over 80 and distance to the first region affected, humidity variables (AH or dew point)  
12 retained a negative association with R0 (continent-specific spline p-values were 0.0915 (North  
13 America) and 0.0988 (South Europe) for AH, respectively 0.0506 and 0.1078 for dew point  
14 temperature). The relationship between R0 and mean temperature was markedly different between  
15 North America (negative association, p=0.005) and South Europe (p=0.17).

## 16 Discussion

17

### 18 Summary

19 In this study, we analysed SARS-CoV-2 propagation parameter R0 during the first wave of the pandemic  
20 in 63 regions of 6 north western countries. We showed that R0 values were influenced by population  
21 density (+0.6 for a 10-fold increase in density), by proximity with the first epidemic focus of the country  
22 or coast for USA (-0.3 for a 10-fold increase in distance to the first region to record 10 COVID-19  
23 deaths), and by weather or climate conditions. For regions with mean temperatures below 10°C during  
24 the transmission period, a linear association was observed with R0 values: a difference between  
25 regions of +1°C was associated with a 0.16-unit decrease in R0. A difference in mean absolute humidity  
26 of +1 g/m<sup>3</sup> was associated with a 0.15-unit decrease in R0. Similar results were obtained with dew  
27 point temperatures, with a difference of 1°C was associated with a 0.08-unit decrease in R0 (Table S5).  
28 After adjusting for major confounders and spatial autocorrelation, our results indicate that weather  
29 conditions brought a significant contribution to drive the magnitude of the first wave, even if it was  
30 limited by an initial heterogeneous spread of the virus, which protected regions located furthest away  
31 from the first foci.

32

### 33 Strength and limits

34 This study relied on a regional scale analysis and accounted for different dynamics within the same  
35 country. The overall epidemic wave at country level was actually the sum of diverse dynamics, as is  
36 obvious for large countries but also true for Spain, Italy or France, where regions were heterogeneously  
37 affected, as confirmed by serological studies [3, 31]. Likewise, weather or climate heterogeneity  
38 between regions of a given country was large. By analyzing distinct spatial units with heterogeneous  
39 population density and weather, we were able to assess the effect of parameters that may be  
40 otherwise confounded by country-level parameters such as response strategy, timing of the analysis  
41 period compared to the progression of the epidemic, but also age structure of the population.

42 The 6 countries were selected due to their homogeneous location in the northern hemisphere  
43 between 25 and 50 degrees of latitude and the low efficacy of their counter epidemic responses until

1 a lockdown was decreed. We are therefore as close as possible of conditions allowing  $R_0$  estimation.  
2 This 4-parameter hierarchical generalized additive model provides an explanation of up to 45% of  $R_0$   
3 variability across 63 affected regions of the northern hemisphere, thus providing useful insights on the  
4 drivers of the first wave, and allowing to estimate the contribution of population density and weather  
5 conditions for the next waves, when the effect of local introduction is no longer relevant.

6 We acknowledge several limits. The first one is the necessity to rely on death counts to estimate  $R_0$   
7 during this wave due to the lack of information on actual infections from limited testing and the lack  
8 of consistency between countries for hospitalization counts. This assumption is similar to usual  
9 assumptions for  $R_0$  estimation based on diagnosed cases, since true number of infections remains  
10 unknown and detection occurs at variable delays after infection but it could have led to an  
11 underestimation of the  $R_0$ . Indeed, while the average delay between infection and death was 3 weeks,  
12 deaths occurring from infections contracted the same day may in fact occur over a larger window  
13 extending several weeks beyond this delay.

14 The second one is the use of a single summary weather observation over the assumed transmission  
15 period, which may fail to express the dynamical aspects of weather. The choice of fixed, 1-week  
16 increments to study the effect variations in the weather summary window may be too coarse to  
17 capture effects for narrow exponential growth periods. The sensitivity analysis showed a slight increase  
18 in effect when considering weather summary values calculated 1 week earlier than the estimated  
19 transmission period, but the 18-day sensitivity analysis showed a stronger negative relationship  
20 between  $R_0$  and AH summary values corresponding to 1-week later than the estimated transmission  
21 period. The role of the weather conditions might be more important during the beginning of the  
22 exponential growth period, until a sufficiently large number of persons becomes infected and  
23 parameters such as population density become increasingly important. This study could also only  
24 evaluate the effect of a limited range of weather conditions on SARS-CoV-2 transmission, since the  
25 number of observations with a mean temperature below  $2.5^\circ\text{C}$  or above  $15^\circ\text{C}$  was low. This prevents  
26 from analyzing the effect of higher temperatures such as during autumn. This restriction was however  
27 necessary to achieve a minimal homogeneity of the studied regions in terms of their exposure and  
28 response to the pandemic. Finally, this analysis includes only 63 regions and may lack statistical power.  
29 The necessity to ensure that the epidemic growth of deaths was sufficient led to the exclusion of  
30 regions that may be affected, but not enough for daily deaths counts to reach 10 deaths/day.

31 Finally, this study showed an association between SARS-CoV-2  $R_0$  and temperature/absolute humidity,  
32 but due to the strong correlation between absolute humidity and temperature in the seasonal  
33 conditions analysed here, it is difficult to determine which parameter is more important and they could  
34 not be analysed in combination [30]. The continent-specific analysis suggests that the relationship  
35 between absolute humidity and  $R_0$  was more stable than that of temperature, which was strong in the  
36 US but less so in South Europe. We could not conclude whether the relationship results from a direct  
37 role of weather on individual susceptibility to viral invasion (*e.g.* dry nasal mucosa from indoors heating  
38 and outdoors cold) or on viral persistence/survival, or from an indirect role of climate on human  
39 behaviors (*e.g.* regions with cold winter favor more indoors living conditions and lead to bigger  
40 infection opportunities).

#### 41 **Conclusion**

42 Our study shows an important dependency of SARS-CoV-2 transmission to weather/climate, with a  
43 0.16-unit increase in  $R_0$  for a  $1^\circ\text{C}$  difference in mean regional temperature below  $10^\circ\text{C}$ , or a 0.15-unit  
44 increase for a  $-1\text{g}/\text{m}^3$  decrease in absolute humidity. Northern hemisphere countries experienced a  
45 second wave of SARS-CoV-2 infections during autumnal transition from summer to winter, while still  
46 actively maintaining control strategies. Public health strategies need to account for a further increase

1 in transmissibility when/where cold and dry winter conditions are reached. In the regions of the north-  
2 west hemisphere, lifting restrictions on social activities during the winter would likely lead to faster  
3 increases than observed during the second wave, when autumnal conditions were prevalent.

4

#### 5 **Authors' contribution**

6 JL, JG, SC and AF designed the study. JL conducted the analysis with methodological contributions of  
7 JP, EL, and LL. JL JP EL LL AF SC JG contributed to interpreting the results and editing the manuscript.

8

#### 9 **Acknowledgements**

10 The authors would like to thank Laurax Simgiane Ferbliegas from Hab' lab Marseille and L. Jae for  
11 help and support in retrieving multi-country regional data.

## 1   References

- 2   1. Flaxman S, Mishra S, Gandy A, Unwin HJT, Mellan TA, Coupland H, et al. Estimating the effects of  
3   non-pharmaceutical interventions on COVID-19 in Europe. *Nature*. 2020;584:257–61.
- 4   2. Cauchemez S, Kiem CT, Paireau J, Rolland P, Fontanet A. Lockdown impact on COVID-19 epidemics  
5   in regions across metropolitan France. *The Lancet*. 2020;396:1068–9.
- 6   3. Pollán M, Pérez-Gómez B, Pastor-Barriuso R, Oteo J, Hernán MA, Pérez-Olmeda M, et al.  
7   Prevalence of SARS-CoV-2 in Spain (ENE-COVID): a nationwide, population-based seroepidemiological  
8   study. *Lancet*. 2020;396:535–44.
- 9   4. Lai C, Wang J, Hsueh P. Population-based seroprevalence surveys of anti-SARS-CoV-2 antibody : An  
10   up-to-date review. *Int J Infect Dis*. 2020;101:314–22.
- 11   5. Moriyama M, Hugentobler WJ, Iwasaki A. Seasonality of Respiratory Viral Infections. *Annu Rev*  
12   *Virol*. 2020;7:83–101.
- 13   6. Matson MJ, Yinda CK, Seifert SN, Bushmaker T, Fischer RJ, Doremalen N Van, et al. Effect of  
14   Environmental Conditions on SARS-CoV-2 Stability in Human Nasal Mucus and Sputum. *Emerg Infect*  
15   *Dis*. 2020;26:9–11.
- 16   7. Morris DH, Claude Yinda K, Gamble A, Rossine FW, Bushmaker T, Fischer RJ, et al. Mechanistic  
17   theory predicts the effects of temperature and humidity on inactivation of SARS-CoV-2 and 2 other  
18   enveloped viruses. *bioRxiv*. 2020.
- 19   8. Briz-Redón Á, Serrano-Aroca Á. The effect of climate on the spread of the COVID-19 pandemic: A  
20   review of findings, and statistical and modelling techniques. *Prog Phys Geogr*. 2020;44:591–604.
- 21   9. Gillibert A, Jaureguiberry S, Hansmann Y, Argemi X, Landier J, Caumes E, et al. Comment on A.  
22   annua and A. afra infusions vs. Artesunate-amodiaquine (ASAQ) in treating *Plasmodium falciparum*  
23   malaria in a large scale, double blind, randomized clinical trial. *Phytomedicine*. 2019; in press:152981.
- 24   10. Mecnas P, da Rosa Moreira Bastos RT, Rosário Vallinoto AC, Normando D. Effects of  
25   temperature and humidity on the spread of COVID-19: A systematic review. *PLoS One*. 2020;15 9  
26   September:1–21.
- 27   11. Azuma K, Kagi N, Kim H, Hayashi M. Impact of climate and ambient air pollution on the epidemic  
28   growth during COVID-19 outbreak in Japan. *Environ Res*. 2020;190:110042.
- 29   12. Rubin D, Huang J, Fisher BT, Gasparrini A, Tam V, Song L, et al. Association of Social Distancing,  
30   Population Density, and Temperature With the Instantaneous Reproduction Number of SARS-CoV-2  
31   in Counties Across the United States. *JAMA Netw open*. 2020;3:e2016099.
- 32   13. Merow C, Urban MC. Seasonality and uncertainty in global COVID-19 growth rates. *Proc Natl*  
33   *Acad Sci U S A*. 2020;117:27456–64.
- 34   14. Baker RE, Yang W, Vecchi GA, Metcalf CJE, Grenfell BT. Susceptible supply limits the role of  
35   climate in the early SARS-CoV-2 pandemic. *Science (80- )*. 2020;369:315–9.
- 36   15. Saad-roy CM, Wagner CE, Baker RE, Morris SE, Farrar J, Graham AL, et al. Immune life history,  
37   vaccination, and the dynamics of SARS-CoV-2 over the next 5 years. *Science (80- )*. 2020;818  
38   November:811–8.
- 39   16. Zaitchik BF, Sweijd N, Shumake-Guillemot J, Morse A, Gordon C, Marty A, et al. A framework for  
40   research linking weather, climate and COVID-19. *Nat Commun*. 2020;11:19–21.
- 41   17. Wiersinga WJ, Rhodes A, Cheng AC, Peacock SJ, Prescott HC. Pathophysiology, Transmission,  
42   Diagnosis, and Treatment of Coronavirus Disease 2019 (COVID-19): A Review. *JAMA - J Am Med*  
43   *Assoc*. 2020;324:782–93.
- 44   18. Bi Q, Wu Y, Mei S, Ye C, Zou X, Zhang Z, et al. Epidemiology and transmission of COVID-19 in 391

- 1 cases and 1286 of their close contacts in Shenzhen, China: a retrospective cohort study. *Lancet Infect*  
2 *Dis.* 2020;20:911–9.
- 3 19. Richardson S, Hirsch JS, Narasimhan M, Crawford JM, McGinn T, Davidson KW, et al. Presenting  
4 Characteristics, Comorbidities, and Outcomes among 5700 Patients Hospitalized with COVID-19 in  
5 the New York City Area. *JAMA - J Am Med Assoc.* 2020;323:2052–9.
- 6 20. Grasselli G, Greco M, Zanella A, Albano G, Antonelli M, Bellani G, et al. Risk Factors Associated  
7 With Mortality Among Patients With COVID-19 in Intensive Care Units in Lombardy, Italy  
8 Supplemental content. *JAMA Intern Med.* 2020;180:1345–55.
- 9 21. ISCIII. Informe sobre la situación de COVID-19 en España. 2020.
- 10 22. Istituto Superiore di Sanità. Characteristics of SARS-CoV-2 patients dying in Italy Report based on  
11 available data on December 16th , 2020. 2020.
- 12 23. Zhou F, Yu T, Du R, Fan G, Liu Y, Liu Z, et al. Clinical course and risk factors for mortality of adult  
13 inpatients with COVID-19 in Wuhan, China: a retrospective cohort study. *Lancet.* 2020;395:1054–62.
- 14 24. Worldpop, Department of Geography and Geosciences University of Louisville, Department de  
15 Geographie Universite de Namur, CIESIN Columbia University. Global High Resolution Population  
16 Denominators Project. 2018. <https://www.worldpop.org/doi/10.5258/SOTON/WP00647>. Accessed  
17 25 Jun 2020.
- 18 25. Lolli S, Chen YC, Wang SH, Vivone G. Impact of meteorological conditions and air pollution on  
19 COVID-19 pandemic transmission in Italy. *Sci Rep.* 2020;10:1–15.
- 20 26. Google LLC. Google COVID-19 Community Mobility Reports.  
21 [https://www.google.com/covid19/mobility/data\\_documentation.html?hl=en](https://www.google.com/covid19/mobility/data_documentation.html?hl=en). Accessed 4 Sep 2020.
- 22 27. Salje H, Kiem C, Lefrancq N, Courtejoie N, Paireau J, Andronico A, et al. Estimating the burden of  
23 SARS-CoV-2 in France To cite this version : HAL Id : pasteur-02548181. 2020.
- 24 28. Wallinga J, Lipsitch M. How generation intervals shape the relationship between growth rates and  
25 reproductive numbers. *Proc R Soc B Biol Sci.* 2007;274:599–604.
- 26 29. Obadia T, Haneef R, Boëlle P. The R0 package : a toolbox to estimate reproduction numbers for  
27 epidemic outbreaks. 2012.
- 28 30. Babin S. Use of Weather Variables in SARS-CoV-2 Transmission Studies. *Int J Infect Dis.*  
29 2020;100:333–6.
- 30 31. Warszawski J, Bajos N, Meyer L, de Lamballerie X, Seng R, Beaumont A-L, et al. In May 2020, 4.5%  
31 of population in metropolitan France developed antibodies against SARS-CoV-2: first results from  
32 the national survey EpiCov [french]. 2020.

1 **Tables**

2 **Table 1: Multivariable model results for the relationship between R0 and weather parameters,**  
 3 **obtained with the hierarchical generalized additive model.** Weather parameters are temperature,  
 4 absolute humidity, and dew point temperature, adjusted for distance to the first region affected,  
 5 population density, and elderly population. Non-linear effects are presented in Figure 6. Models  
 6 assuming linear effects for weather covariates are presented in Table S5.

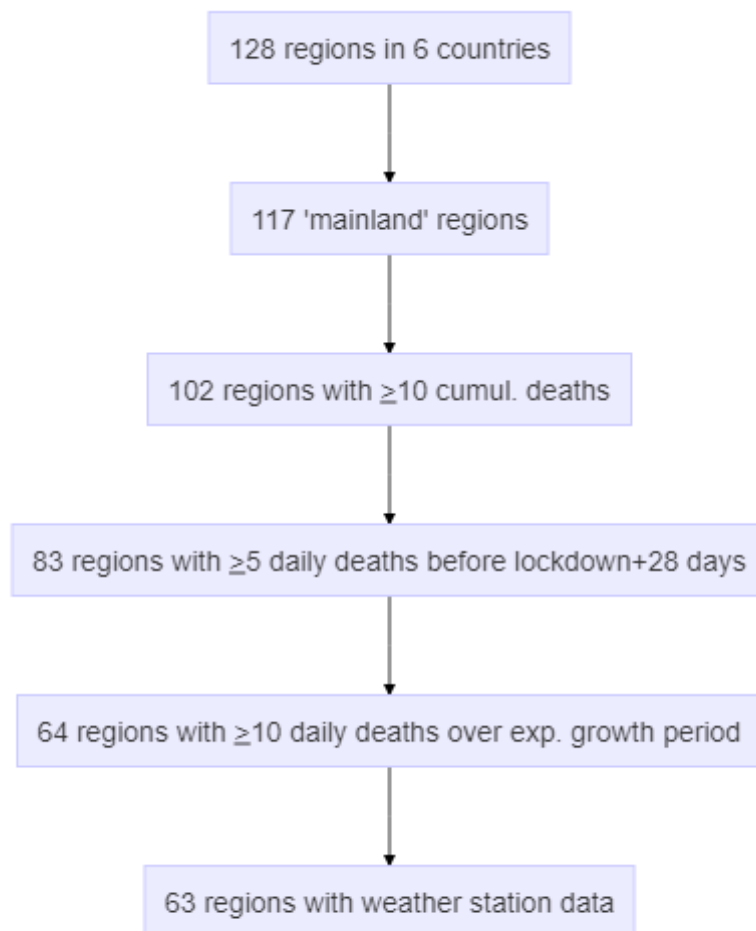
7

Model	Variable	Estimate	95%CI	p-value
<b>Model 1</b>	Intercept	0.78	[-0.88 - 2.45]	0.36152
	Population density (log10)	0.67	[0.07 - 1.26]	0.03218
	% population over 80	0.05	[-0.08 - 0.18]	0.44470
	Distance to first region affected in the country/coast	<b>spline</b>		0.08007
	<b>Mean temperature</b>	<b>spline</b>		0.00655
	Dev. explained: 41.5%			
<b>Model 2</b>	Intercept	1.28	[-0.36 - 2.92]	0.13239
	Population density (log10)	0.50	[-0.11 - 1.11]	0.11294
	% population over 80	0.03	[-0.1 - 0.16]	0.61862
	Distance to first region affected in the country/coast	<b>spline</b>		
	<b>Mean AH</b>	<b>spline</b>		0.03401
	Dev. explained: 33.6%			
<b>Model 3</b>	Intercept	1.20	[-0.47 - 2.88]	0.16427
	Population density (log10)	0.49	[-0.12 - 1.1]	0.12005
	% population over 80	0.05	[-0.08 - 0.18]	0.47092
	Distance to first region affected in the country/coast	<b>spline</b>		0.09756
	<b>Mean Dew Point Temperature</b>	<b>spline</b>		0.00494
	Dev. explained: 34.6%			

8

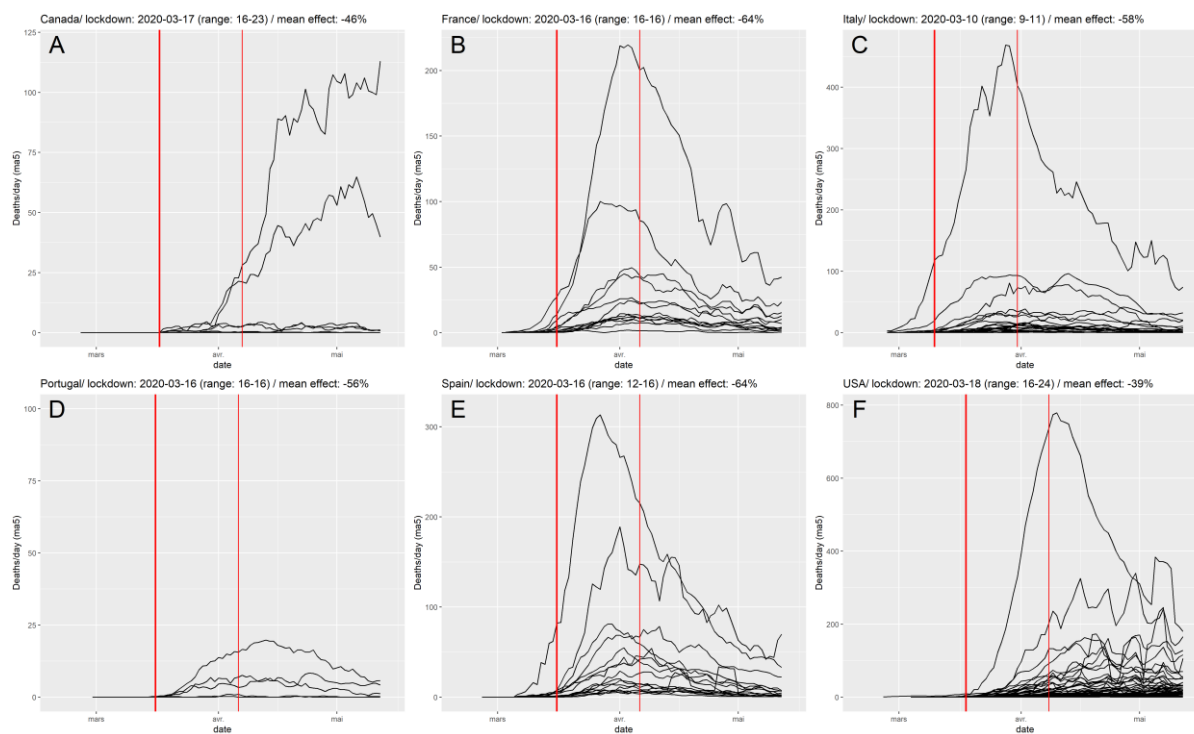
1 **Figures**

2 **Figure 1: Study flow chart**



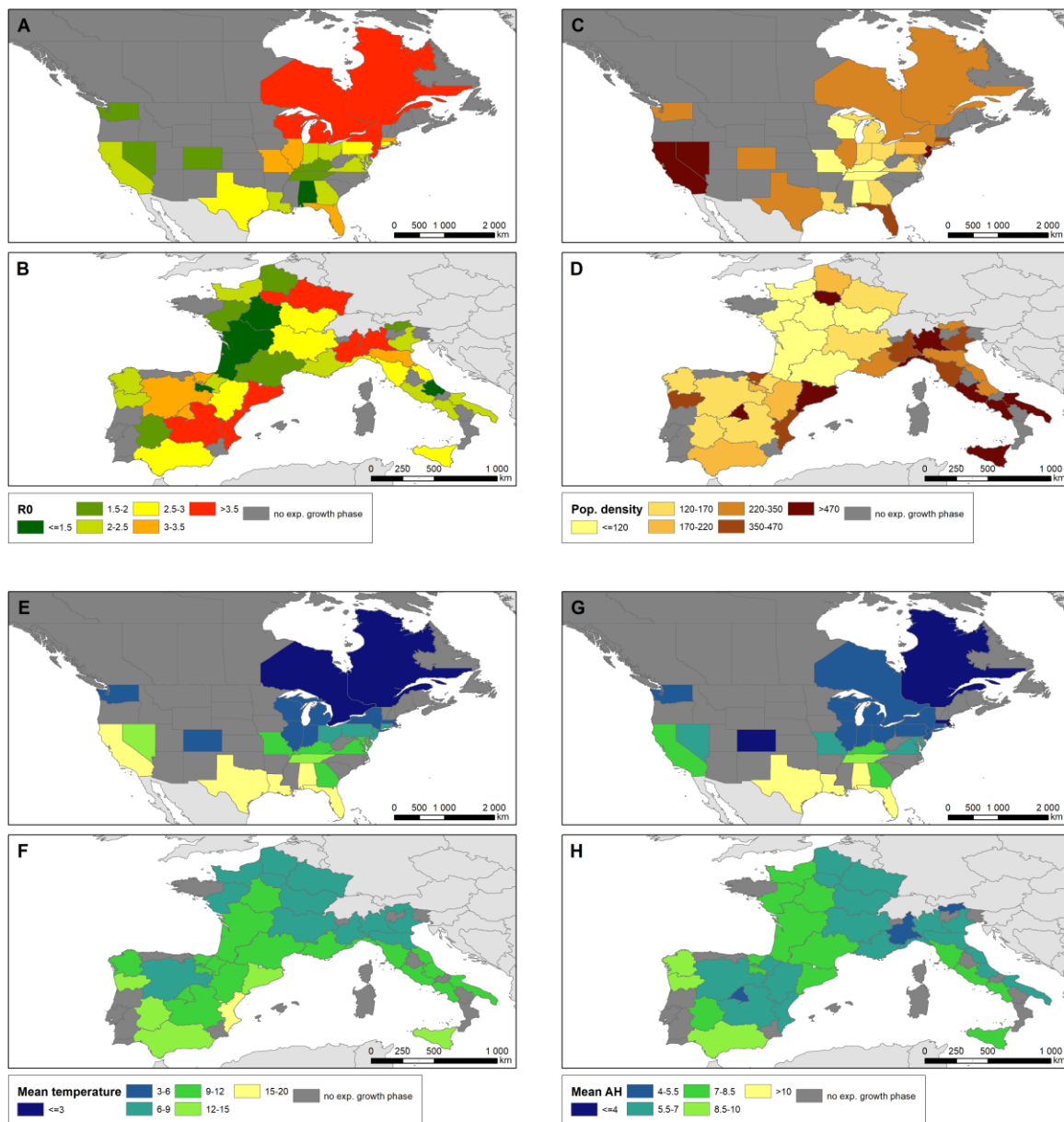
3

1 **Figure 2: Deaths per day, by region and by country.** The thick red line figures the median date of  
2 lockdown by each country, and the thin red line the median date +28 days.



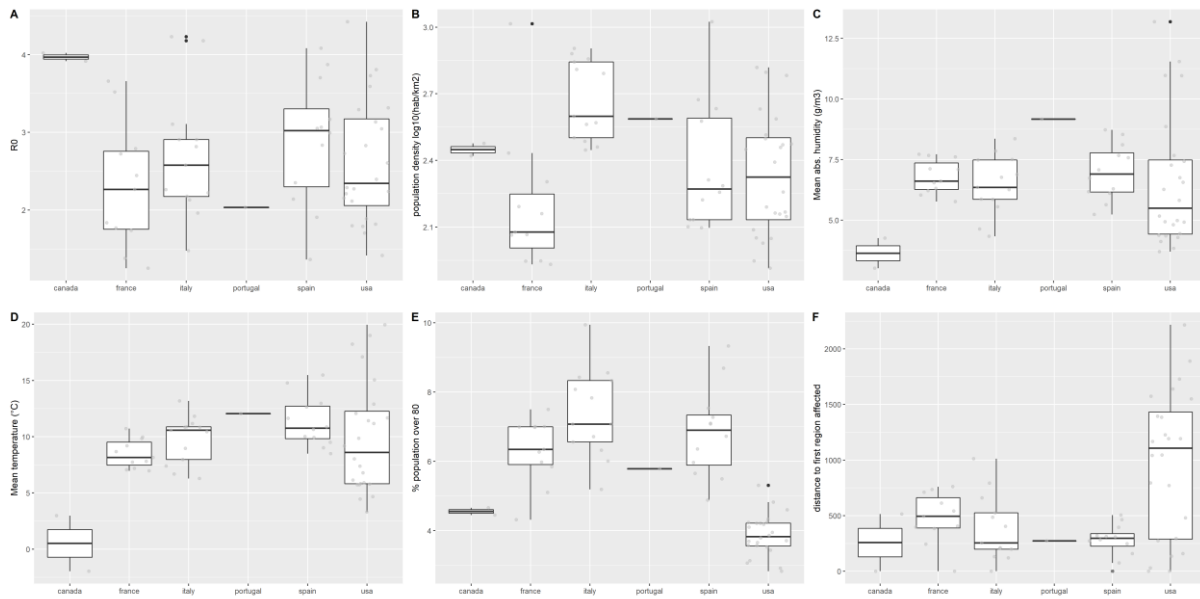
3

1 **Figure 3: Map of regional values for R0 and selected covariates, panels are presented by continent.**  
 2 A,B: R0 ; C,D: population density (inhabitants per km2) ; D,E: mean temperature ; F,G: mean absolute  
 3 humidity.



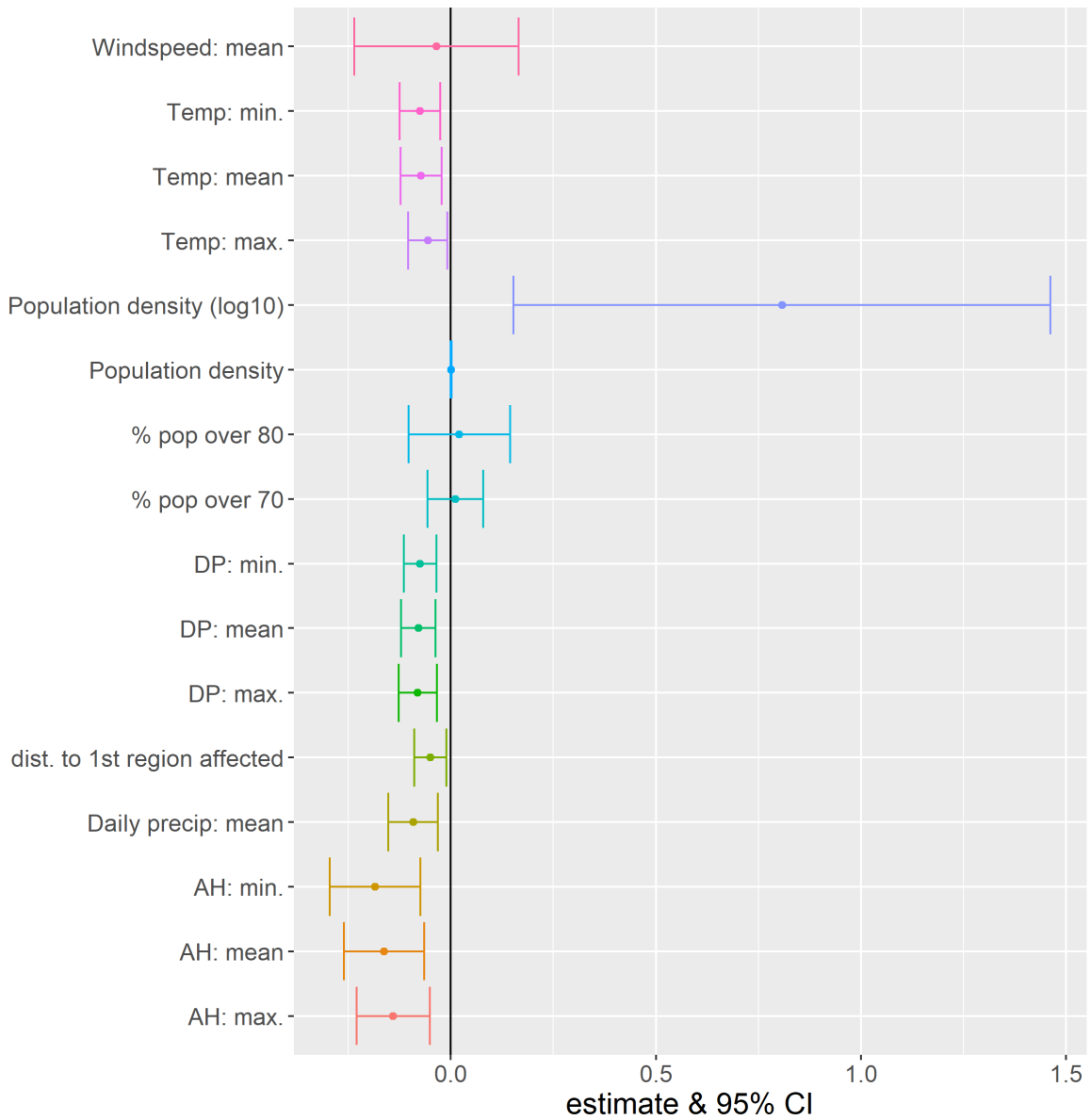
4

- 1 **Figure 4: Distribution of R0 and selected covariates by country.** A: R0; B: population density (log10 inhabitants/km2); C: Mean absolute humidity (g/m3); D: Mean temperature (°C); E: Population over 80 years old (%); F: distance to the first region affected (km).
- 2
- 3



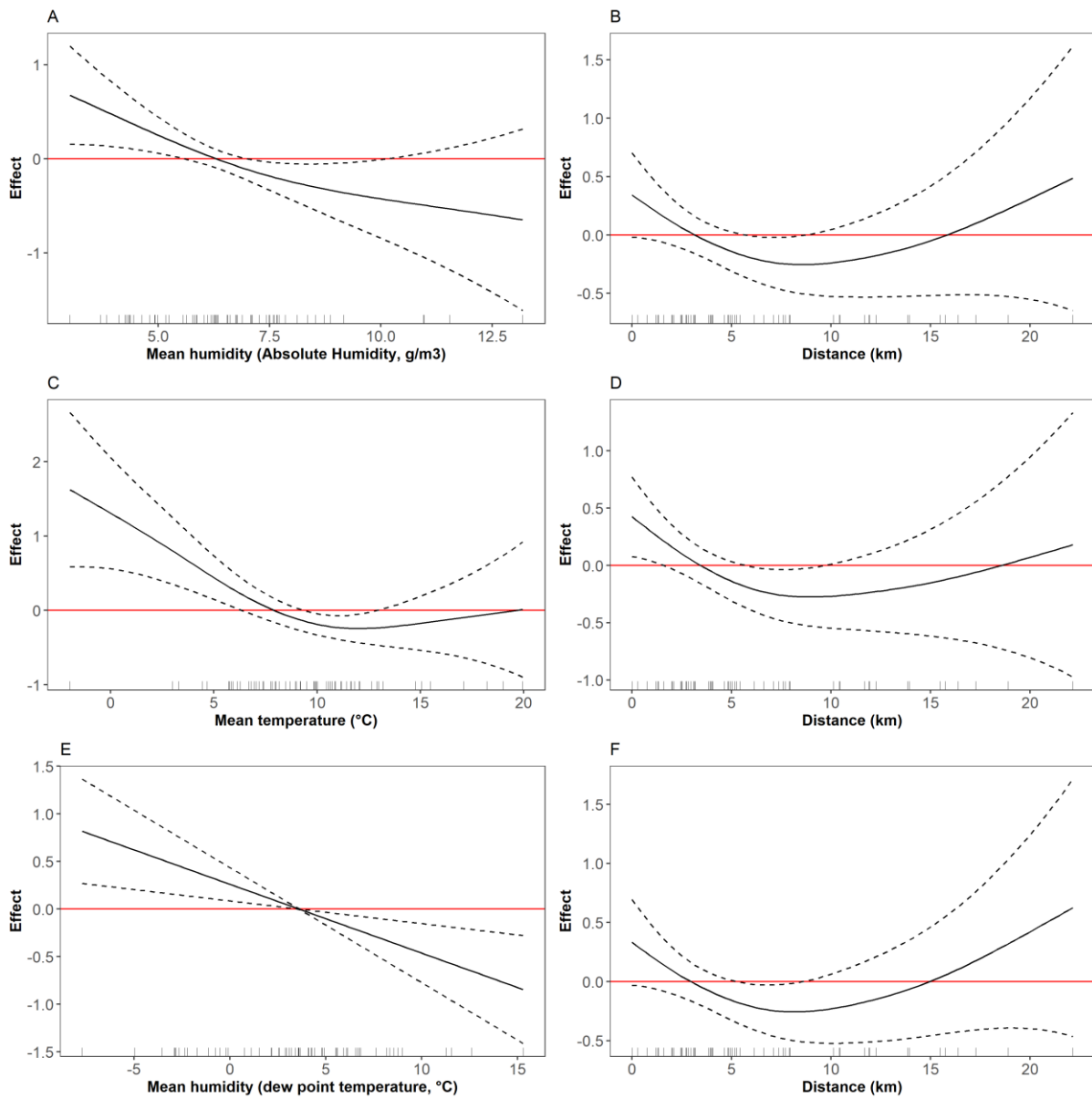
4

1 **Figure 5: Change in R0 on an additive scale estimated from the univariable model assuming a linear**  
2 **relationship between R0 and the different variables.**



3

1 **Figure 6: Non-linear effects in the multivariable model for weather parameters (see Table 1 for linear**  
2 **effects).** A: Temperature, model 1. B: Distance to first region affected, model 1. C: absolute humidity,  
3 model 2. D: distance to first region affected, model 2. E: dew point temperature, model 3. F: distance  
4 to first region affected, model 3.



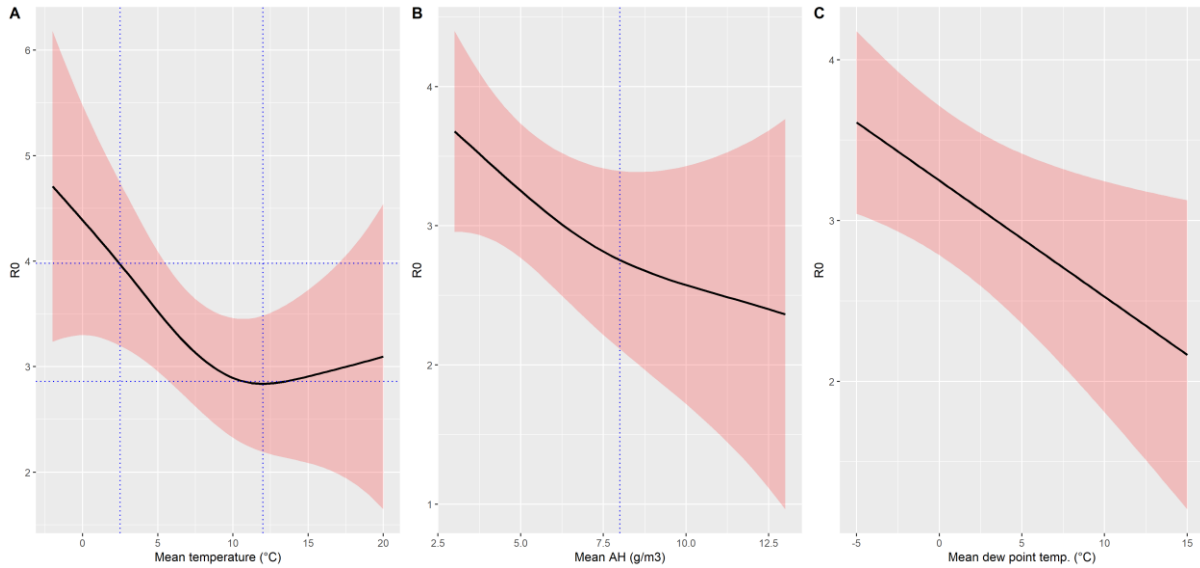
5

6

1 **Figure 7: Summary of estimated effect of temperature (A), absolute humidity (B) or dew point**  
2 **temperature (C) on  $R_0$  assuming a region with average population density (248 persons/km<sup>2</sup>) and**  
3 **percentage of inhabitants >80 years (5.6%), and corresponding to the first region first affected**  
4 **(distance=0km).**

5

6



7